IEEE Access
Multidisciplinary | Rapid Review | Open Access Journal

Received June 5, 2020, accepted June 22, 2020, date of publication June 29, 2020, date of current version September 8, 2020.

Digital Object Identifier 10.1109/ACCESS.2020.3005717

An Adaptive Sine-Cosine Moth-Flame Optimization Algorithm for Parameter Identification of Hybrid Active Power Filters in Power Systems

YUFAN WU, RONGLING CHEN, CHUNQUAN LI, (Member, IEEE), LEYINGYUE ZHANG, AND WANXUAN DAI

School of Information Engineering, Nanchang University, Nanchang 330029, China

Corresponding author: Rongling Chen (rongling_chen@163.com)

This work was supported in part by the National Natural Science Foundation of China under Grant 61863028, Grant 61503177, and Grant 81660299, in part by the China Scholarship Council under the State Scholarship Fund under Grant CSC 201606825041, in part by the Science and Technology Department of Jiangxi Province of China under Grant 20161ACB21007, Grant 20171BBE50071, and Grant 20171BAB202033, and in part by the Education Department of Jiangxi province of China under Grant GJJ14228 and Grant GJJ150197.

ABSTRACT Hybrid active power filter (HAPF) is a novel technique of harmonic filter which combines superiorities of both active and passive filters. However, extracting appropriate parameters of the HAPF, including active filter gain, passive inductive, and capacitive reactance within a constraint space is still a challenging task. To obtain more accurate parameters of HAPF, this paper proposed a new population-based algorithm named ASC-MFO. In ASC-MFO, the swarm is divided into two sub-swarms, i.e., exploitation group and the exploration group. The exploitation group adopts the SFM in the MFO algorithm to enhance the exploitation ability, while the exploration group utilizes the SCM in the SCA algorithm to emphasize exploration. Besides, a personal best flame generation (PFG) strategy and a hybrid exemplar generation (HEG) strategy are developed for the exploitation group and the exploration group to further enhance the exploitation ability and the exploration ability of the two subgroups, respectively. Moreover, an adaptive strategy is proposed to automatically resize the population number of two sub-swarms during the iterative process, which can precisely balance the exploration and exploitation ability between groups in every single generation. The proposed ASC-MFO is applied to design the two most commonly used topologies of the HAPF, where each topology contains four actual cases. Comprehensive experimental results demonstrate that ASC-MFO obtains an excellent performance among those well-established algorithms, especially in the aspect of accuracy and reliability.

INDEX TERMS Sine cosine algorithm (SCA), moth flame optimization (MFO), swarm Global optimization, hybrid active power filter (HAPF).

I. INTRODUCTION

With the advancement of science and the development of technology, an increasing number of nonlinear loads are being connected to the power system, which leads to an exponential increase of harmonic pollution (HP). Obviously, a high degree of HP responsible for the low quality of power. This problem affects the operation of the electric power sector to varying degrees. In the worst situation, this problem shuts the whole factories down [1]– [3].

Passive power filters PPF is the first adopted technique for reducing or eliminating HP. It is a combination of capacitive and inductive pairs, and the different sizes of capacitors and inductors result in different frequency response characteristics of PPF. Thus, it is simple to use with a relatively low economical cost, which enables PPF to become the most commonly used technology for harmonic suppression [4]–[6]. However, the static frequency response of PPF cannot catch

The associate editor coordinating the review of this manuscript and approving it for publication was Ran Cheng.

up with the dynamic changes of nonlinear loads. Moreover, an accurate PPF requires an accurate · and specific capacitive and inductive pair, while the capacitors and inductors provided by current manufacturers all have errors, and the values are determined.

On the other hand, active power filters (APF) are more reliable and acquire better performance than PPF [7]. The active shunt filter acts as a harmonic compensator and injects the current in anti-phase with the distortion components present in the line current. In contrast, the series active filter acts as a harmonic isolator [8]. However, APF has not been widely used because of its high cost and delicate operation compared with traditional PPF. The hybrid active power filter (HAPF) is proposed, which combines passive and active power filters with several topologies. Compared with pure APF, HAPF has a much smaller size and rating. While compared with pure PPF, it can overcome most of the problems in PPF and remove the resonance which may occur. Nevertheless, the design of the HAPF is considered a complex problem, which makes HAPF not widely available. To be more specific, the parameter gain value of HAPF is usually determined based on experiments [9], and the values of capacitance and inductance values are still hard to choose due to the nonlinearity of the load.

The meta-heuristic methods have been widely used in recent years to solve all kinds of practical engineering problems. For example, parameter extracting problems of PV system [10] and Trajectory planning problem [11]. Natural phenomena inspire most of these algorithms, and these methods aim at finding an optimal of an objective function within a predefined search space. Compared with the traditional gradient-based approaches, these methods are considered insensitive to solution space and easy to apply [12]–[14]. Some scholars use these meta-heuristic methods to designed the filters in the power system. For example, predator-prey based firefly optimization [15], ant colony optimization [16], particle swarm optimization [17], ant direction hybrid DE [18], genetic algorithms [19], bacterial foraging optimization [20], etc. However, most of these methods are applied to design PPF; a small number of meta-heuristic methods are used to design HAPF. When designing HAPF with these methods, most of the objective functions are formulated with multiple optimization objectives [9], [21], which increase the search difficulty and computational burden of these algorithms. Reference [22] proposed an optimal design of two popular topologies of HAPF, which formulated the objective function with a single objective, and adopted an L-SHADE algorithm to designed the HAPF. The objective function formulated in [22] reducing the difficulty of designing HAPF. In consideration of the objective function is multimodal with several local optimal, developing a new meta-heuristic algorithm to optimize HAPF is necessary to obtain a better performance.

The Moth-flame optimization (MFO) algorithm was first proposed by Seyedali Mirjalili in 2015 [23]. It is one of the recently proposed meta-heuristic methods inspired by the navigation mechanism of moths in nature. MFO begins with a determined quantity of artificial moths and artificial flame; then, each moth flies to its corresponding flame with a spiral trajectory. After a certain number of iterations, MFO can find the best flame, which represents the best solution in the search space. MFO adopts a competition mechanism to select the promising flames and retain the flame with low fitness value, resulting in the fast convergence of moth around the flame with the best solution. Meanwhile, the spiral trajectory allows moths to adequately explore the space around the best solution, which guarantees MFO a good exploitation ability. Because of the above advantages, MFO was widely applied in practical engineering problems, such as multilevel thresholding image segmentation [24], accurate simulation of a non-uniform electric field [25], Parameter Identification of Single-Phase Inverter [13]. However, as a newly developed meta-heuristic algorithm, some problems existed in MFO that still need to be addressed, such as accuracy and exploration ability. More specifically, the flames abandoned during the earlier search process may guide the moths to a more promising solution region while the flames reserved during the later search process suffer a diversity loss problem. In other words, once the flames are concentrated in the optimum local area, MFO has difficulty using an existing strategy to escape from this space. Thus, the accuracy of the MFO algorithm is not guaranteed once flames are locked in an optimum local area, and the exploitation ability of the MFO algorithm is weak due to the flames suffer a diversity loss problem in the iterative process.

To solve the above problems, some MFO variants are proposed to overcome the deficiency of MFO. Li C *et al.* proposed a double evolutionary moth-flame optimization (DELMFO) algorithm, which adopted an evolutionary flame generation strategy [14]. Soliman *et al.* proposed two improved MFO algorithms, with two newly designed spiral trajectories for moths around flames [26]. In [27], a Lévy-fight moth-fame algorithm was developed, where Lévy-fight strategy is adopted to increase the diversity of moths during the search process. Nevertheless, according to no free lunch theory [28], no algorithm can resolve all the optimization problems. Especially in the problem of obtaining accurate parameters of HAPF, most of the state-of-art meta-heuristic algorithms fall into a local optimal. Thus, designing a new MFO variant to accurate abstract parameters of HAPF is of great significance.

The Sine-Cosine Algorithm (SCA) is involved in the MFO algorithm to improve the performance of the MFO algorithm in this work. SCA is also a recently developed meta-heuristic algorithm proposed by Seyedali Mirjalili in 2016, which can resolve a variety of practical engineering problems [29]. The SCA algorithm adopts a sine-cosine mechanism (SCM) which can randomly choose a sine or cosine trajectory for the exemplar to follow. These two trajectories allow individuals to search towards or away from the exemplar, which makes the SCA algorithm features a high exploration ability when compared with the MFO algorithm. However, the SCM

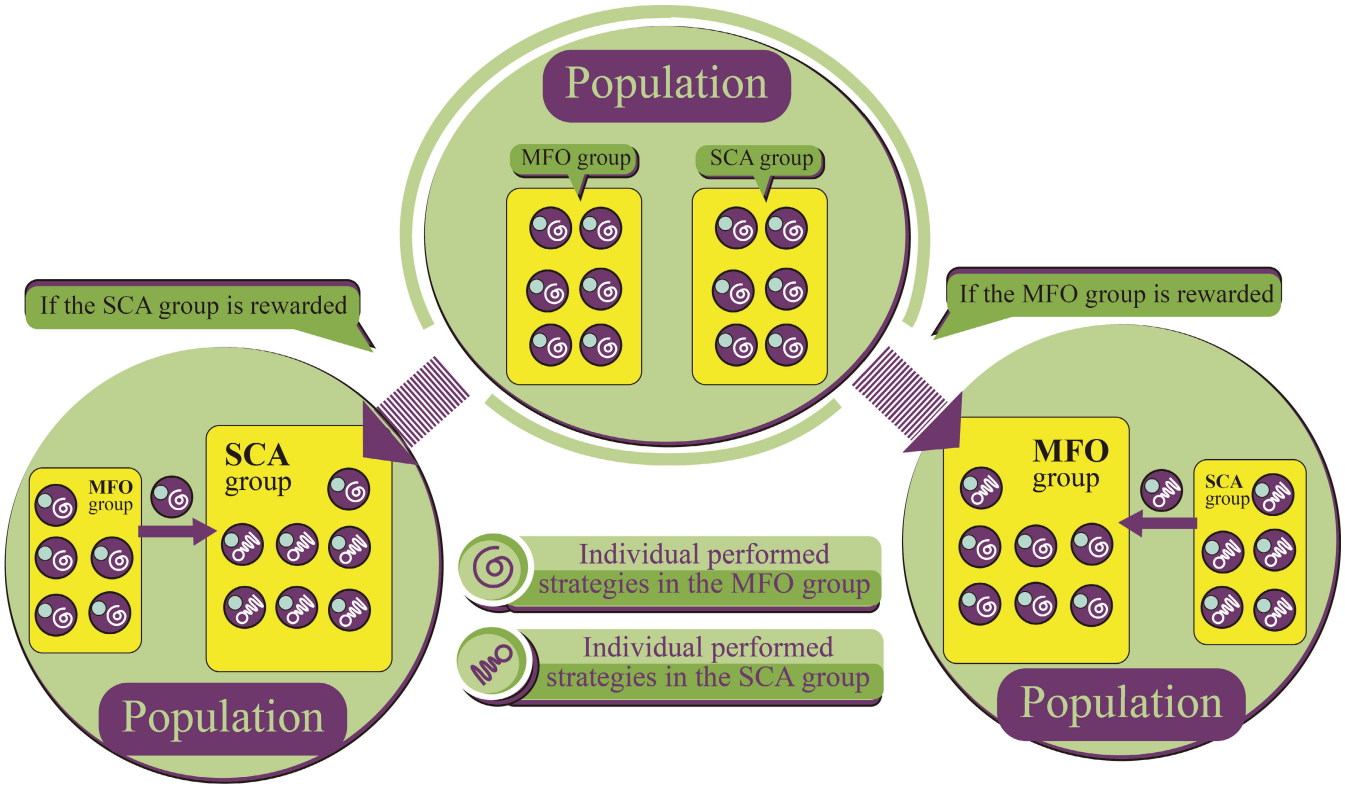

FIGURE 1. The framework of our proposed ASC-MFO algorithm.

slows down the convergence speed, which contributes to a low exploration ability of the SCA algorithm. This paper proposed an Adaptive Sine-cosine Moth-Flame Optimization (SCA-MFO) algorithm. MFO features high exploitation ability while the SCA features high exploitation ability. Thus, the ASC-MFO algorithm aims to integrate the advantages of both MFO and SCA algorithms. In the ASC-MFO algorithm, the swarm is divided into two parallel working subswarm, i.e., exploitation group and the exploration group. The exploitation group adopts the SFM in the MFO algorithm to emphasize on exploitation. In contrast, the exploration group adopts the SCM in the SCA algorithm to obtain the ability of exploration. The swarm division can preserve the diversity of ASC-MFO during the whole iterative process. To generate high-quality flames in the exploitation group, a personal best flame generation (PFG) strategy is proposed. The PFG strategy generates flames from the personal best pool. Compared with the SFUM strategy in the MFO algorithm, The PFG strategy can select flames from the exploration group which is considered with high exploitation ability. Thus, The PFG strategy can enhance the exploitation ability of the exploitation group. Meanwhile, a hybrid exemplar generation (HEG) scheme is adopted for the exploration group. HEG will generate an exemplar from the hybrid population. Thus, individuals in the exploration group have a large probability to explore around an exemplar generated from the exploitation group, which ensures the high exploration ability of the exploration group. Moreover, instead of predefined sizes of subpopulation groups, we developed an adaptive method to regulate the population size of both the MFO group and the SCA group automatically. Our swarm adaptive mechanism (SAM) will be executed in every single generation. Meanwhile, a set of rules for rewards and punishments are designed to adjust the subswarm size of our proposed ASC-MFO automatically. Then a subpopulation size limitation is offered to ensure the two subswarms co-work in a reasonable swarm size. Fig.1 illustrates the swarm adaptive mechanism. The proposed ASC-MFO is utilized to designed HAPF and compared with other well-established algorithms. Comprehensive experimental results demonstrate that ASC-MFO obtained an outstanding performance when compared with its competitors. Note that DELMFO is the most recently proposed competitive MFO variants [14], L-SHADE is a competitive algorithm which obtains an excellent performance on designing HAPF [22].

The main contributions of this paper are as follows:

1) This paper proposed an Adaptive Sine-cosine Moth-Flame Optimization Algorithm (ASC-MFO) algorithm, which firstly integrates the advantages of both MFO and SCA. In the proposed ASC-MFO algorithm, the swarm is divided into two subswarm, i.e., exploitation group and exploration group, which focus on exploitation and exploration, respectively. The exploitation group adopts the spiral flight mechanism in the MFO algorithm, and the exploration group utilizes the sine-cosine mechanism in the SCA algorithm.

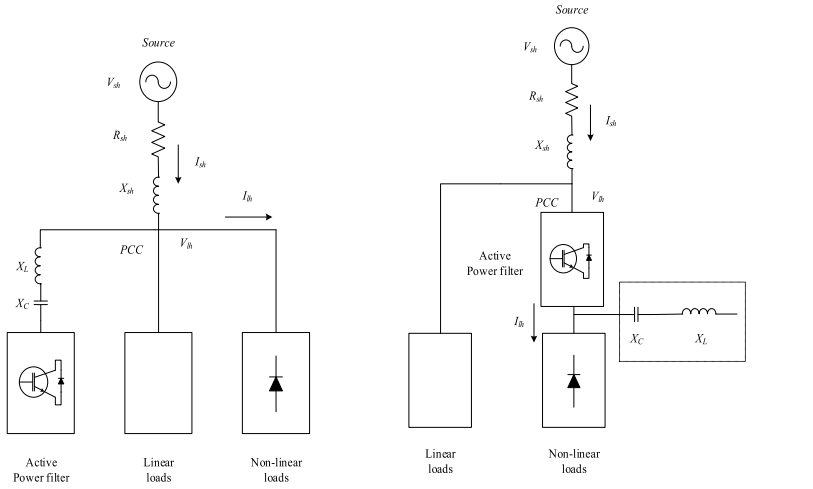

(a) APF in series with shunt passive filter (b) Combined series APF and shunt passive filter

FIGURE 2. Circuit model of two popular HAPF topologies.

The swarm division can preserve the diversity of ASC-MFO during the whole iterative process.

2) A personal best flame generation (PFG) strategy and a hybrid exemplar generation (HEG) strategy are developed for the exploitation group and the exploration group, respectively. PFG aims to provide high-quality flames, which ensure the high exploitation ability of the exploitation group; the HEG strategy aims to generate a promising exemplar from the hybrid population, which ensures the high exploration ability of the exploration group. The implement of both PFG and HEG strategy balance the exploitation ability and the exploration ability of the proposed ASC-MFO algorithm.

3) A swarm size adaptive mechanism (SAM) with a new set of reward and punishment rules is proposed to adjust the subswarm size of our proposed ASC-MFO, which performs in each iterative generation with a population size limitation. This mechanism can precisely adjust the exploitation ability and the exploration ability of the proposed ASC-MFO algorithm, and the population size limitation can preclude the diversity loss of population in case of the overuse of SAM.

4) The proposed ASC-MFO is firstly applied to develop two popular conditions of the HAPF in the power system, i.e., series topology and parallel topology. Then, ASC-MFO is compared with other well-established algorithms on these HAPF topologies. Comprehensive experimental results indicate that the proposed ASC-MFO can obtain accurate parameters and outperform its competitors.

The following article is organized as follows. Section II gives two popular HAPF model and formulates the single objective function; Section III briefly introduces the original MFO algorithm and SCA algorithm; Section IV proposed an ASC-MFO algorithm; Section V analyzes the overall experimental results; Section VI makes a brief conclusion.

II. PROBLEM FORMULATION

A. TWO POPULAR TOPOLOGIES OF HAPF

Fig.2 gives two popular topologies of HAPF. Fig.2(a) represents the 'APF in series with passive shunt filter' while Fig.2(b) denotes the 'combined series APF and shunt passive filter', respectively. Both of them are widely used for compensation in industrial power systems. In Fig.2, R_{sh} and X_{sh} represents the transmission system resistance and inductive reactance in ohms at harmonic 'h', respectively; R_{lh} and X_{lh} denotes load resistance and inductive reactance in ohms at harmonic 'h' respectively; 'K' means controllable feedback gain of HAPF on ohms; X_L and X_C indicates fundamental inductive and capacitive reactance in ohms of the passive filter; I_s and I_l represents the Root mean square (RMS) value of supply current and load current in amperes, respectively; V_s and V_L denotes the RMS value of supply voltage and load voltage (line-to-neutral), respectively. In the power system, the point of common coupling (PCC) is usually taken as the point closest to the user where the system owner or operator could offer service to another user [30]. In Fig.2(a), the active filter eliminates load harmonics by injecting harmonic currents, improving the performance of passive filters. In Fig.2(b), series APF provides high-impedance power supply harmonics and forces the currents of harmonic to flow to the passive filter; thus, low current rating is allowed in APF.

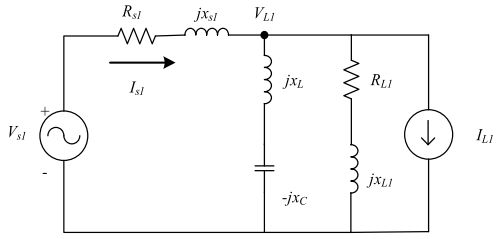

FIGURE 3. Single-phase equivalent circuit at fundamental frequency (h = 1).

Fig.3 is the single-phase equivalent circuit applicable for both HAPF topologies at the fundamental frequency [31]. Subject 1 means the circuit model works at the fundamental frequency. The single-phase equivalent circuits of the two topologies at harmonic frequencies are different. They can

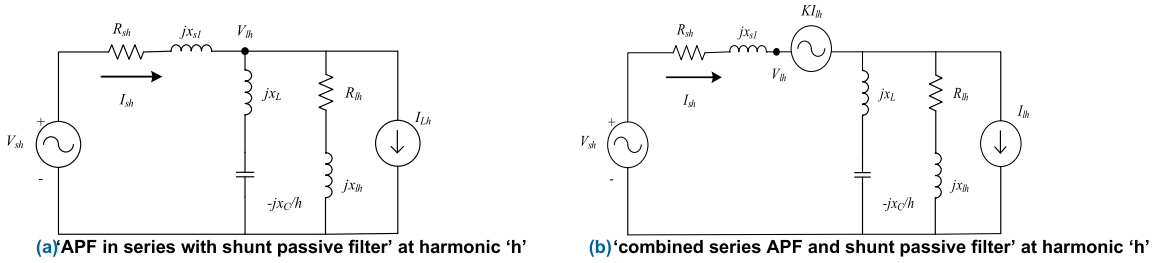

(a) 'APF in series with shunt passive filter' at harmonic 'h' (b) 'combined series APF and shunt passive filter' at harmonic 'h'

FIGURE 4. Single-phase equivalent circuit at harmonic 'h'.

be formulated in Fig.4(a) and Fig.4(b), which denotes the 'APF in series with shunt passive filter' and 'combined series APF and shunt passive filter' at harmonic 'h', respectively. In Fig.4, APF serves as a controlled voltage source, which is proportional to the supply current, i.e., $V_{APF} = KI_{sh}$. The filter gain K is designed to provide zero impedance at the fundamental frequency [32], which means APF acts as a harmonic resistor.

The utility supply voltage and the nonlinear load can be represented by Thevenin voltage source and the harmonic current source, respectively [32]:

$$V_s(t) = \sum\nolimits_h V_{sh}(t) \tag{1}$$

$$I_L(t) = \sum\nolimits_h I_{lh}(t) \tag{2}$$

The *h-th* harmonic source and load impedance can be formulated as:

$$Z_{lh} = R_{sh} + jX_{sh} \tag{3}$$

$$Z_{lh} = R_{lh} + jX_{lh} \tag{4}$$

Thus, the load admittance is

$$Y_{lh} = G_{lh} + jB_{lh} \tag{5}$$

where G_{lh} and B_{lh} represent the load resistance and inductive reactance in ohms and loads conductance and susceptance in mho at harmonic 'h'. The compensated utility supply current and load voltage at harmonic '$h > 2$' in Fig.4(a) can be expressed as fractions, respectively:

$$I_{sh} = \frac{A + jB}{C + jD} \tag{6}$$

$$V_{lh} = \frac{E + jF}{C + jD} \tag{7}$$

Similarly, the compensated utility supply current and load voltage at harmonic 'h>2' in Fig.4(b) can be expressed as:

$$I_{sh} = \frac{A + jB}{C + jD'} \tag{8}$$

$$V_{lh} = \frac{E + jF}{C + jD'} \tag{9}$$

where,

$$A = V_{sh}R_{lh} - I_{lh}X_{lh}(hX_l - \frac{X_c}{h}) \tag{10}$$

$$B = V_{sh}\left(X_{lh} + hX_l - \frac{X_c}{h}\right) + I_{lh}R_{lh}(hX_L - \frac{X_c}{h}) \tag{11}$$

$$R_{TLh} = R_{sh}R_{lh} - X_{sh}X_{lh} \tag{12}$$

$$D = X_{TLh} + KX_{lh} + (R_{sh} + R_{lh})(hX_L - \frac{X_c}{h}) \tag{13}$$

$$X_{TLh} = R_{lh}X_{sh} + R_{sh}X_{lh} \tag{14}$$

$$E = V_{sh}\left[KR_L - X_{lh}\left(HX_L - \frac{X_c}{h}\right)\right] + I_{lh}X_{TLh}(hX_L - \frac{X_c}{h}) \tag{15}$$

$$F = V_{sh}\left[KX_{lh} - R_{lh}\left(HX_L - \frac{X_c}{h}\right)\right] + I_{lh}R_{TLh}(hX_L - \frac{X_c}{h}) \tag{16}$$

$$D' = X_{TLh} + KX_{lh} + (K + R_{sh} + R_{lh})(hX_L - \frac{X_c}{h}) \tag{17}$$

$$F' = V_{sh}\left[KX_{lh} + (K + R_{lh})\left(hX_L - \frac{X_c}{h}\right)\right] - I_{lh}R_{TLh}(hX_L - \frac{X_c}{h}) \tag{18}$$

Eq (6) and eq (8) reveal that the active filter serves as a damping resistance [32], which means no amplification of the current occurs at different harmonic level h. Meanwhile, the power filter gain K is inverse proportional to the compensated utility supply current I_{sh}, which means the increase of the gain K results in a decreasing of source harmonic current. On the other hand, a high gain K may result in a high compensated PCC voltage V_{Lh} according to eq (7) and eq (9). Thus, our objective is to find a gain K which keeps both V_{Lh} and I_{sh} at a low level.

Other system parameters are given as follow:

$$DPF = \frac{P_{l1}}{V_{l1}I_{s1}} = \frac{G_{l1}V_{l1}}{I_{s1}} \tag{19}$$

where DPF represents the compensated load-displacement power factor, ad '1' means the fundamental component.

$$PF = \frac{P_l}{V_l I_s} = \frac{G_{l1}V_{l1}^2 + \sum_{h\geq 2} G_{lh}V_{lh}^2}{\left(I_{s1}^2 + \sum_{h\geq 2} I_{sh}^2\right)\left(V_{l1}^2 + \sum_{h\geq 2} V_{lh}^2\right)} \tag{20}$$

where PF represents the compensated load power factor.

$$P_{LOSS} = I_{s1}^2 R_{s1} + \sum\nolimits_{h\geq 2} I_{sh}^2 R_{sh} \tag{21}$$

where P_{LOSS} denotes Transmission Loss.

$$\eta = \frac{P_l}{P_l + P_{LOSS}} \tag{22}$$

where η denotes transmission efficiency.

$$VTHD = \frac{\sqrt{\sum_{h\geq 2} V_{lh}^2}}{V_{l1}} \tag{23}$$

$$ITHD = \frac{\sqrt{\sum_{h\geq 2} I_{sh}^2}}{V_{s1}} \tag{24}$$

where *VTHD* and *ITHD* indicate compensated voltage and compensated utility supply current.

Then the harmonic pollution (HP) can be mathematically modeled as:

$$HP = \sqrt{VTHD^2 + ITHD^2} \tag{25}$$

B. OBJECTIVE FUNCTION FORMULATION

To ensure *VTHD* and *ITHD* within the harmonic limits, the objective function for optimization is formulated as:

$$HP_{APP} = abs\left(VTHD_{lim} - VTHD\right) + abs\left(ITHD_{lim} - ITHD\right) \tag{26}$$

where,

$VTHD_{lim}$ = limitation on *VTHD* prescribed by IEEE 519-2014 [31] based on system voltage level,

$ITHD_{lim}$ = limitation on *ITHD* prescribed by IEEE 519-2014 [31] based on system short circuit ratio.

While meeting individual harmonics within IEEE standard limitation, the function of objective optimization is obtained:

$$\text{Maximize } `HP_{APP}' \quad \text{subject to } PF = PFgoal \pm \varepsilon \tag{27}$$

where *PFgoal* is the desired power factor, and ε denotes an error value to promote the iterative process. In this work, '$-HP_{APP}$' is input as an objective function that is to be minimized by optimizing K, X_c and, X_L. Then, an OBJ_{temp} is set to replace the fitness value of a determined K, X_c, and X_L value.

III. RELATED WORK

A. MFO ALGORITHM

Moth-flame optimization (MFO) algorithm was proposed by Seyedali Mirjalili in 2015 [22], which models the navigation behavior of moths. In the MFO algorithm, each candidate solutions are represented by moths, and these moths can be initialized as:

$$M = [m_1, m_2, \ldots, m_n, \ldots, m_N] \tag{28}$$

$$m_n = [m_{n1}, m_{n2}, \ldots, m_{nd}, \ldots, m_{nD}] \tag{29}$$

$$m_{nd} = m_{ld} + r_d \cdot (m_{ud} - m_{ld}) \tag{30}$$

$$OM = \left[fun(m_1), fun(m_2), \ldots, fun(m_n), \ldots, fun(M_N)\right] \tag{31}$$

where M is a matrix that consists of moths; m_n denotes the number n_{th} moths and N is the population size of the hole swarm; D is the maximum number of dimensions, and m_{nd} denotes the d_{th} dimension of the n_{th} moth; m_{ud} and m_{ld} represents the upper and lower bound of candidate solutions, respectively; r_d is randomly generated within [0,1], and $fun(*)$ is an operator which can acquire a fitness value corresponding to its operand moth.

Flames play an essential role in the search process of MFO. Similar to the initialization of moths, the flames can be formulated as:

$$\mathcal{F} = [f_1, f_2, \ldots, f_n, \ldots, f_N] \tag{32}$$

$$f_n = [f_{n1}, f_{n2}, \ldots, f_{nd}, \ldots, f_{nD}] \tag{33}$$

$$O\mathcal{F} = \left[fun(f_1), fun(f_2), \ldots, fun(f_n), \ldots, fun(f_N)\right] \tag{34}$$

where $\mathcal{F}$ contains N flames, f_n denotes the n_{th} flame, and each flame is regarded as a candidate solution with D components. $fun(F)$ represents the fitness value of the flames. Each flame can find its corresponding fitness value in $fun(F)$.

In every single generation, moths fly to its corresponding flame with a spiral trajectory. The Spiral flight mechanism (SFM) is formulated as follows:

$$S\left(m_i, f_j\right) = \left|m_i - f_j\right| \cdot \mathrm{e}^{bt} \cdot cos2\pi t + f_j \tag{35}$$

where M_i and $\mathcal{F}_j$ indicate the i_{th} moth and its corresponding j_{th} flame, b is a constant that defines the shape of the spiral trajectory as a logarithmic spiral, and t is a random number within $[-1, 1]$.

Then, the flames will be updated by the SFUM:

$$O\mathcal{F}_{k+1} = sort(P_k)_n \tag{36}$$

$$P_k = \begin{pmatrix} OM_k \\ O\mathcal{F}_k \end{pmatrix} \tag{37}$$

where k denotes the current iteration number, and $k+1$ means the next iteration, $sort(P_k)_n$ is an operator that sort the elements of the vector P_k from small to large and retains the first n elements, P_k indicates a vector that splicing the vector OM and $O\mathcal{F}$ in the k_{th} iteration in a column. $O\mathcal{F}$ and $\mathcal{F}$ are one-to-one correspondences. In other words. $\mathcal{F}$ is determined once the $O\mathcal{F}$ vector is obtained.

The number of flames steps down with the iteration number increase, and the flame numbers can be calculated as:

$$\text{fn} = RO\left[maxfn - \frac{k \cdot (maxfn - 1)}{maxit}\right] \tag{38}$$

where *maxit* indicates the max iteration number, *maxfn* means the max or the initialized number of flames, $RO(*)$ is an operation to make the operand round to its nearest integer.

B. SCA ALGORITHM

Sine Cosine algorithm(SCA) [29] is also proposed by Seyedali Mirjalili in 2016. Without loss of generality, the candidate solutions in SCA are formulated as a matrix:

$$X = \begin{pmatrix} x_{1,1} & x_{1,2} & \cdots & x_{1,d} \\ x_{2,1} & x_{2,2} & \cdots & x_{2,d} \\ \vdots & \vdots & \ddots & \vdots \\ x_{n,1} & x_{n,2} & \cdots & x_{n,d} \end{pmatrix} \tag{39}$$

where such row vector $X_n = [x_{n,1}, x_{n,2}, \ldots, x_{n,d}]$ represents the n-th candidate solution or individual, and n is lower than the population size N; d denotes the dimensional number,

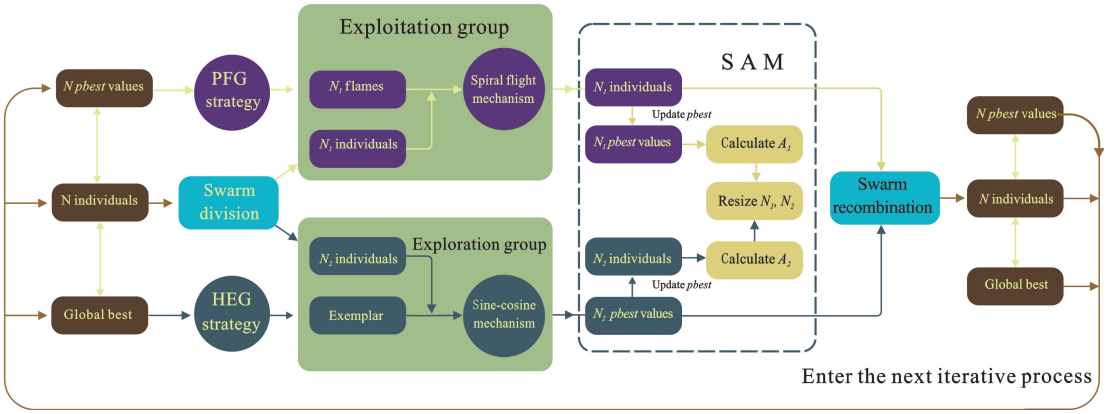

FIGURE 5. The framework of the proposed ASC-MFO algorithm.

and d is lower than the max dimensional number D. Then, each updates its position vector by following a trajectory with sine and cosine function. The sine-cosine mechanism is formulated as:

$$X_n^{k+1} = \begin{cases} X_n^k + r1 * \sin(r2) * \left| r_3 P_n^k - X_n^k \right|, & r4 < 0.5 \\ X_n^k + r1 * cos(r2) * \left| r_3 P_n^k - X_{nn}^k \right|, & r4 \geq 0.5 \end{cases} \quad (40)$$

where P_n^k denotes the personal best solution obtained so far, $r2\epsilon$ [0, 2π] determine the search direction towards or escape from the global best position, r3 is randomly distributed in [0, 2], r4ϵ [0, 1] is a switch for sine or cosine function, $r1$ is linear decreasing with the iterative number increasing, $r1$ is formulated as:

$$r1 = a - t * \frac{a}{T} \quad (41)$$

where a is a constant, t is the current iteration number, and T is the max iteration number. $r1$ balances the exploration and exploitation ability of the SCA in the different stages of the iterative process.

IV. PROPOSED ASC-MFO ALGORITHM

MFO features good exploitation ability because individuals in the MFO algorithm follows its flames by a spiral trajectory according to eq (35). MFO updates its flames with a 'survival of the fittest' mechanism, which means the flames with better fitness value will survive from the flame selection. This mechanism makes the MFO algorithm features a fast convergence speed but also raises a problem of diversity loss of moths. To preserve the diversity of moths and take advantage of the exploitation ability of the MFO algorithm. We try to introduce some methods with strong exploration ability into the MFO algorithm. The sine cosine trajectory in the SCA algorithm is what we expected. According to eq (40), individuals have a chance to search opposite from the vector P_n^k. Once a part of moths flies with sine cosine trajectory, moths have a chance to jump out of the optimal local region, and the diversity of moths is increased. Then, we need to find a particular algorithm structure to combine the MFO algorithm and SCA algorithm to avoid conflicts between these two methods. In HCLPSO [34], the swarm is divided into two sub-swarms. One of the sub-swarms focuses on exploitation, and the other aims at exploration. This swarm partition operator allows two conflicting tasks to exist in one algorithm and co-work together effectively. In this work, swarm partition technology is adopted to balance the strategies in the MFO algorithm and the strategies in the SCA algorithm.

The new proposed algorithm is named as ASC-MFO, and the framework of our new proposed ASC-MFO algorithm is illustrated in Fig.5. To allow SCA and MFO algorithm co-work simultaneously, the swarm in the ASC-MFO algorithm is divided into two parallel working subgroups. The group updated by the SCM in the SCA algorithm is named as the exploration group. Similar to the SCA algorithm, the exploration group follows the SCM, and the exemplar in every single generation will generate from the hybrid population:

$$s_i^{k+1} = \begin{cases} s_i^k + r1 * \sin(r2) * \left| r_3 * gbest^k - s_i^k \right|, & r4 < 0.5 \\ s_i^k + r1 * cos(r2) * \left| r_3 * gbest^k - s_{ii}^k \right|, & r4 \geq 0.5 \end{cases} \quad (42)$$

where s_n^k represents the *i-th* individual in exploration group at the *k-th* generation; $r2 \in [0, 2\pi]$, r3 $\in$ [0, 1] and r4 $\in$ [0, 1] are all randomly generated variables; $r1$ is updated by eq (41); $gbest^n$ denotes the global best position generated from the hybrid population after the population recombination in every single generation (HEG). From eq (42), we can see that individuals in the exploration group only explores or exploits around $gbest^n$; this mechanism helps the exploration group complete its exploration task within a reasonable explore region.

The group updated by the MFO algorithm is called the exploitation group, which means moths in the MFO group focus on exploitation tasks. Different from the flames decreasing methods of eq (38) in the MFO algorithm, flames will not decrease in this subgroup to ensure moths focus on exploitation tasks. Each individual in the exploitation group are called as a moth:

$$\mathcal{F}_n^{k+1} = sort\left(pbest_n^k\right)_{N_2} \quad (43)$$

$$m_n^{k+1} = \left| m_n^k - f_n^k \right| \cdot \mathrm{e}^{bt} \cdot cos2\pi t + f_n^k \tag{44}$$

where eq (43) denotes the new developed PFG strategy; eq (44) represents the SFM in the MFO algorithm; n denotes the *n-th* flames or moths; $Pbest_n^k$ denotes the personal best solution obtained so far; N_2 denotes the group size of exploitation group; since flames in the exploitation group will not decrease with the generation number increase, the *n-th* moth corresponds with its *n-th* flame.

Swarm adaptive mechanism (SAM) in the proposed ASC-MFO algorithm varies with time. SAM will be executed in every single generation, and change one individual when this mechanism is implemented. Meanwhile, a set of rules are devised for rewards and punishments. Each sub-swarm obtained a score after the personal best pool is updated. The sub-swarm with a high updated rate earns a high score, and the sub-swarm with a high score will enlarge its population numbers. The swarm size of the subswarm with a more substantial adaptive value will be increased in the next iteration. Moreover, to prevent population overflows or subpopulations from becoming too large, a subpopulation size limitation *N_lb* is set to ensure the two sub-swarm co-work in a reasonable swarm size. This subswarm size adaptive mechanism is illustrated in Algorithm 1:

Algorithm 1 Subswarm Size Adaptive Mechanism

A1 = cnt1/N1;
A2 = cnt2/N2;
if *A1 > A2*
  N1 = N1 + N_step;
else
  N1 = N1 − N_step;
end if
  N2 = N − N1;
if *N1 > N_ub*
    N1 = N_ub;
  end if
  if *N1 < N_lb*
    N1 = N_lb;
  end if
  A1 = 0; A2 = 0; cnt1 = 0; cnt2 = 0;

where N denotes swarm size; *N_step* determines the change step of subswarm size in every single generation; *A1* and *A2* are adaptive values of exploration subswarm and exploitation subswarm, respectively; *cnt1* and *cnt2* are two counters that count the updating frequency of *pbest* value; In other words, the subswarm with better performance in this particular generation can obtain a higher adaptive value; thus, this subswarm will expand its population size. On the contrary, the swarm size of subswarm with lower adaptive values will decrease due to its bad performance in a particular generation. Nevertheless, there is a limit for both expansion and contraction operator, *N_lb* and *N_ub* define lower bound and upper bound of the size of one subswarm. In this work, *N_step* is set to 1 and 100 in case 4 and other cases, respectively; *N_lb* is set to *10%N*; N_ub is set to *90%N*; Initial swarm size of both subswarm is set to *50%N*;

Algorithm 2 "ASC-MFO Algorithm"

/***Initialization***/
Randomly initialize N individuals into a matrix with N row and D line;
Evaluate the fitness value of each individual;
Initialize *pbest*, *gbest* pool and subswarm size *N1(N2 = N − N1)*;
Clear *A1* and *A2* to zero;
while (end condition is not satisfied) **do**
  iteration = iteration + 1;
/***Update individuals in exploration group***/
  Update *r1* according to eq (41);
  Randomly generate variables *r2*, *r3* and *r4* within its corresponding limit range;
  for i = 1 to *N1* **do**
    Update position vector s_i^k according to eq (42);
    Evaluate the fitness value $f(s_i^k)$;
    Update $pbest_i^k$ and $gbest^k$;
    if $pbest_i^k$ is updated **do**
      cnt1 = cnt1 + 1;
    end if
  end for
/***Update moths in exploitation group***/
  Renew flames according to eq (43);
  for n = 1 to *N2* **do**
    Update moths m_n^k according to eq (44);
    Evaluate the fitness value $f(m_n^k)$;
    Update $pbest_n^k$and $gbest^k$;
    if $pbest_n^k$ is updated **do**
      cnt2 = cnt2 + 1;
    end if
  end for
/***Perform subswarm size adaptive mechanism***/
  A1 = cnt1/N1;
  A2 = cnt2/N2;
  if *A1 > A2*
    N1 = N1 + N_step;
  else
    N1 = N1 − N_step;
  end if
    N2 = N − N1;
  if *N1 > N_ub*
    N1 = N_ub;
  end if
  if *N1 < N_lb*
    N1 = N_lb;
  end if
    A1 = 0; A2 = 0;
end while

Finally, the ASC-MFO algorithm is fully established. The pseudo-code of the proposed ASC-MFO algorithm is displayed in Algorithm 2, and the flow chart is shown in Fig.6.

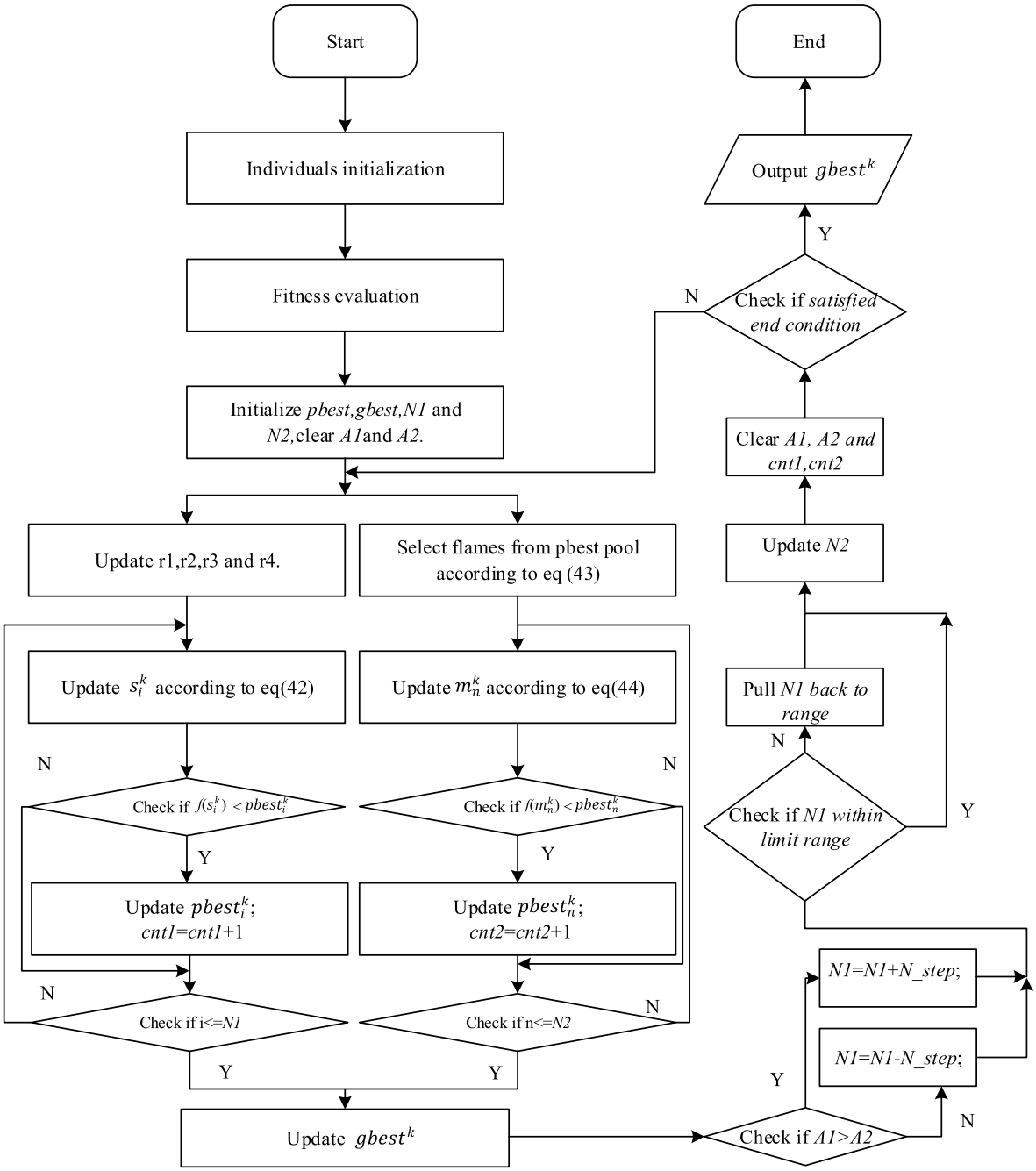

FIGURE 6. Flow chart of the proposed ASC-MFO algorithm.

V. ANALYSIS OF THE EXPERIMENTAL RESULTS

The proposed ASC-MFO algorithm is used to identify three parameters from two popular HAPF topologies, i.e., APF in series with passive shunt filter (series topology) and Combined series APF and shunt passive filter (parallel topology). Our research is based on four case studies. The first three cases are derived from reference [32], where these cases are obtained from an industrial plant, and they are simulated by using the FFSQP optimization method. The numerical data were taken from an example in the IEEE publication [30], where the inductive three-phase loads are 5100KW and 4965 KVAR with a displacement load power factor of 71.65%, and the short-circuit capacity is 80MVA. The fourth case is derived from the reference [22]. All four cases are listed in Table 1. The source and load harmonics are assumed to be time-invariant quantities load, and source resistances are independent of frequency, i.e., $R_{sh} = R_s$ and $R_{Lh} = R_L$. Similar to the reference [22], The $PFgoal$ is set to 95%. Meanwhile, both $VTHD_{lim}$ and $ITHD_{lim}$ are set to 5% based on experimental data. The OBJ_{temp} is set to 1 in

TABLE 1. Four case studies of an industrial plant [22], [32].

Parameters	Case 1	Case 2	Case 3	Case 4
$R_{s1}(\Omega)$	0.02163	0.02163	0.02163	0.02163
$X_{s1}(\Omega)$	0.2163	0.2163	0.2163	0.2163
$R_{L1}(\Omega)$	1.7421	1.7421	1.7421	1.7421
$X_{L1}(\Omega)$	1.696	1.696	1.696	1.696
$V_{s1}(kV)$	2.40	2.40	2.40	2.40
$V_{s5}(\%V_{s1})$	0.00	2.00	4.00	4.00
$V_{s7}(\%V_{s1})$	0.00	1.50	3.00	3.00
$V_{s11}(\%V_{s1})$	0.00	1.00	2.00	3.00
$V_{s13}(\%V_{s1})$	0.00	0.50	1.00	1.20
$I_{L5}(\%I_L)$	40.00	40.00	40.00	40.00
$I_{L7}(\%I_L)$	6.00	6.00	6.00	6.00
$I_{L11}(\%I_L)$	2.00	2.00	2.00	2.00
$I_{L13}(\%I_L)$	1.00	1.00	1.00	1.00

this work, and a high OBJ_{temp} value indicates a low tolerance of bad results that obtained by a single run time of these algorithms.

To prove the effectiveness of the proposed ASC-MFO algorithm, the same experiments are conducted to some well-established algorithms, i.e., SHADE using a linear population size reduction method (L-SHADE) [33], Moth-Flame Optimization Algorithm (MFO) [23], Sine Cosine Algorithm (SCA) [29], Double Evolutionary Learning Moth-Flame Optimization (DELMFO) [14], Heterogeneous comprehensive learning particle swarm optimization with enhanced exploration and exploitation (HCLPSO) [34] and Differential Evolution (DE) algorithm [35]. Note that DELMFO is the most recently proposed competitive MFO variants, L-SHADE is a competitive algorithm which obtains an outstanding performance on designing HAPF. To ensure the fairness of this experiment, the FES of these algorithms are all set to 50000 with 30 times run. The parameter set in this study is shown in Table 2. We try to minimize the objective function value to obtain the best parameters, i.e., power gain K, X_L, and X_C; these variables are limited within the following range in terms of Ohmic values [22]:

- $0 \leq K \leq 20$
- $0 \leq X_C \leq 10$
- $0 \leq X_L \leq 1$

TABLE 2. Parameter settings for well-established algorithms.

Algorithms	Parameter Settings
DELMFO	CR=0.7,σ=0.15, R = rand (),∂=0.6
DE	CR = 0.5, F = 0.5
HCLPSO	$g1$=30, $g2$=20, $c1$=2.5-0.5, $c2$=0.5-2.5, c=3-1.5
SCA	a=2
MFO	b=1
L-SHADE	NP = 100
ASC-MFO	N_step=1, N_lb=10%N, N_ub =90%N

A. EXPERIMENTAL RESULT OF SERIES TOPOLOGY

Table 3 gives the experimental results of all listed algorithms in 30 independent runs. Note that Harmonic pollution (HP) is directly linked to the objective function of this optimization problem. The objective function values (min) represent the accuracy. While the mean objective function values (mean) reflects the average accuracy, and SD is the standard deviation of objective function values and reflects the reliability of the estimated parameters. Total time represents the total time of 30 independent runs in a specific case. Note that this experiment is conducted on a computer with AMD Ryzen 5 2600X Six-core @3.6GHz and 16G RAM.

From Table 3, we can observe that in terms of accuracy, all algorithms get the same minimum value in all four cases except SCA (did not reach the minimum value in all four cases) and HCLPSO (did not reach the minimum value in case 3 and case 4). In terms of average accuracy, the proposed ASC-MFO algorithm ranked first in all cases. HCLPSO algorithm ranked second in case 1 and case 2. SCA algorithm ranked 2 in case3, and DELMFO ranked 2 in case 4. In terms of reliability, the proposed ASC-MFO algorithm ranked first in case 1 and case 2, while LSHADE and DE rank first in case 3 and case 4, respectively. In total CPU times, L-SHADE ranked first in all four cases, and the proposed ASC-MFO algorithm obtained an acceptable rank between the MFO algorithm and the SCA algorithm.

Fig.7 gives boxplots to show the distribution of objective function value results obtained by different algorithms. Note that the symbols "+" in Fig.7 indicate the outlier; The red line in the middle of the blue rectangle represents a median number; The top and bottom of the blue rectangle indicates the lower quartile number and upper quartile number, respectively; Solid lines on both sides of the rectangle means the lower limit and upper limit. Apparently, the lower limit number, upper limit number, lower quartile number, upper quartile number, and median number of the proposed ASC-MFO algorithm are overlapped in the lowest position, which demonstrates the accuracy and average accuracy of ASC-MFO algorithm. Also, there are no outliers of the proposed ASC-MFO algorithm in case 1, case 2, and cas4. In case 3, there are only a few outliers, which indicates the reliability of the proposed ASC-MFO algorithm.

Fig.8 gives the convergence curves of different algorithms by using the average objective function values of the 30 independent runs. It can be derived from Fig.8 that the proposed ASC-MFO achieves a considerable convergence speed and an accurate convergency value.

These above comprehensive comparisons between well-established algorithms and the proposed ASC-MFO algorithms indicate that the proposed ASC-MFO algorithm features effective performance in abstract parameters of series topology, especially in terms of accuracy, average accuracy, and reliability.

Table 4 gives the optimized results and the calculated value of the series topology by using the proposed ASC-MFO algorithm. Note that these calculated results are calculated by equations in section 2. Through further observation, we can observe that with the increase of the harmonic level in the applied voltage, the harmonic pollution is on a rising trend. Actually, the increase of harmonic pollution is closely related to the increase of *ITHD* and *VTHD*. Moreover, a higher level

TABLE 3. Comparisons on the statistical results of different algorithms in four cases of series topology.

Case number	Algorithm	Objective function value				Total time(s)
		min	mean	max	SD	
case 1	ASC-MFO	-9.6750	-9.6750	-9.6738	*5.2E-08*	78.1
	SCA	-9.6567	-9.3744	-8.1580	2.9E-01	83.0
	MFO	-9.6750	-9.4270	-9.3208	2.6E-02	71.4
	L-SHADE	-9.6750	-9.5333	-9.3208	3.0E-02	55.7
	HCLPSO	-9.6750	-9.6632	-9.3208	4.0E-03	83.6
	DELMFO	-9.6750	-9.5806	-9.3208	2.5E-02	87.9
	DE	-9.6750	-9.4861	-9.3208	3.1E-02	85.4
case 2	ASC-MFO	-6.7850	-6.7849	-6.7816	3.7E-07	78.8
	SCA	-6.7832	-6.4772	-6.2262	7.0E-02	82.5
	MFO	-6.7850	-6.6023	-6.4630	2.5E-02	70.9
	L-SHADE	-6.7850	-6.7099	-6.4630	1.9E-02	54.5
	HCLPSO	-6.7850	-6.7742	-6.4630	3.3E-03	82.5
	DELMFO	-6.7850	-6.7636	-6.4630	6.5E-03	87.9
	DE	-6.7850	-6.6133	-6.4630	2.6E-02	83.8
case 3	ASC-MFO	-2.0850	-2.0408	-1.7655	1.2E-02	83.2
	SCA	-2.0627	-1.9845	-1.7221	6.8E-03	82.5
	MFO	-2.0850	-1.8061	-1.7385	1.2E-02	70.1
	L-SHADE	-2.0850	-1.7816	-1.6501	6.9E-03	54.6
	HCLPSO	-2.0804	-1.8949	-1.7477	1.9E-02	82.1
	DELMFO	-2.0850	-1.9253	-1.7655	2.6E-02	92.3
	DE	-2.0850	-1.8081	-1.7655	1.2E-02	85.1
case 4	ASC-MFO	-1.1020	-1.0319	1.0000	1.4E-01	79.8
	SCA	-1.0687	-0.9424	1.0000	1.3E-01	82.7
	MFO	-1.1020	-0.3031	1.0000	7.6E-01	69.9
	L-SHADE	-1.1020	-0.2118	1.0000	9.2E-01	54.3
	HCLPSO	-1.0926	-0.2504	1.0000	9.3E-01	82.2
	DELMFO	-1.1020	-0.9996	1.0000	1.7E-01	89.4
	DE	-1.1020	-0.9810	0.1261	2.6E-02	84.9

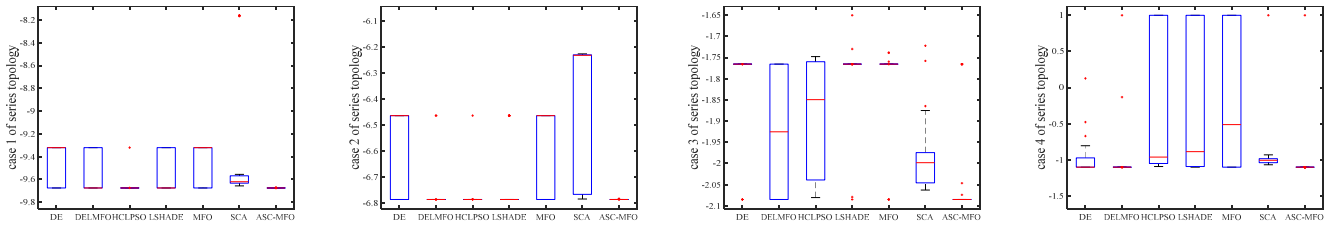

FIGURE 7. Boxplot in 30 runs of different algorithms for four cases of series topology.

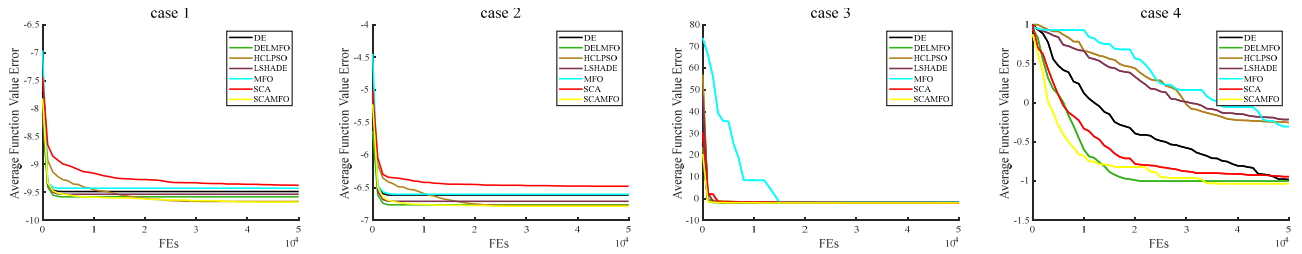

FIGURE 8. Convergence graphs of different algorithms for four cases of series topology.

of harmonic in the applied voltage contributes to a lower gain value K and X_L is almost decreased to zero, which indicates that an active power filter with a low-rated voltage source in series with a passive filter and does not require additional switching filters to eliminate current fluctuations. Besides, all harmonics are found to be within limits as per standard IEEE 519 [30]. The bar chart of I_{Sh} and V_{Lh} is shown in Fig.9.

B. EXPERIMENTAL RESULT OF PARALLEL TOPOLOGY

Table 5 gives the experimental results of all listed algorithms in 30 independent runs of parallel topology. We can see from the table that the proposed ASC-MFO obtained the best min, mean, and SD value, which indicates that the proposed ASCA-algorithm is the most accurate, average accurate, and reliable algorithm. The CPU time cost

TABLE 4. Results for case studies with series topology.

Parameters	Optimization results using ASC-MFO algorithm			
	case 1	case 2	case 3	case 4
$X_C(\Omega)$	2.7094	2.6998	2.6159	2.6187
$X_L(\Omega)$	103.66	91.75	0.00	2.00E-16
$K(\Omega)$	20.00	20.00	9.75	8.47
$PF(\%)$	95.00	95.00	95.00	95.00
$DPF(\%)$	95.00	95.03	95.14	95.18
I_S(A)	753.85	753.55	752.89	752.68
V_L(V)	2430.09	2430.80	2431.87	2432.12
$\eta(\%)$	99.30	99.30	99.30	99.30
P_{LOSS}(kW)	12.29	12.28	12.26	12.25
$ITHD(\%)$	0.200	0.511	3.306	3.898
$VTHD(\%)$	0.125	2.704	4.609	5.000
HP (%)	0.236	2.752	5.672	6.340

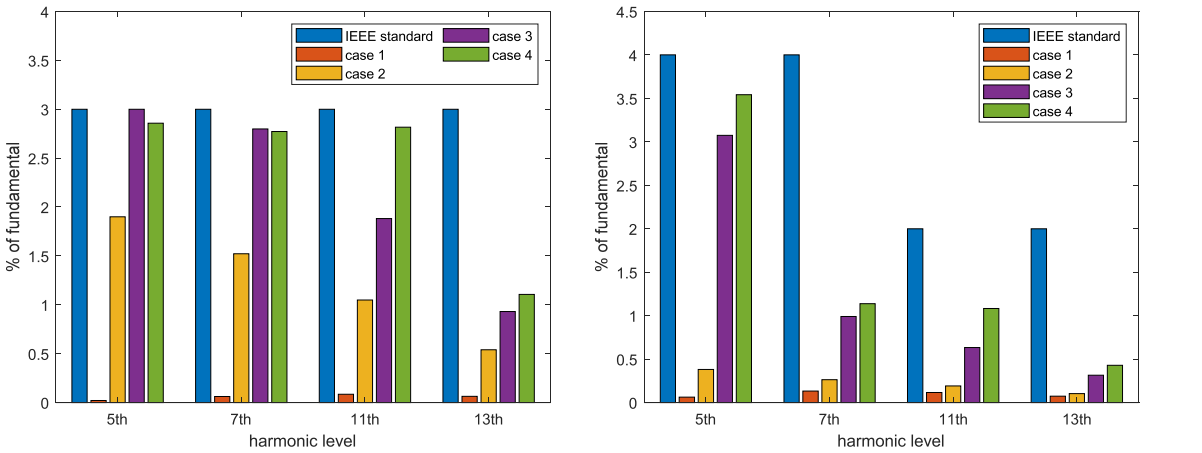

(a)Compensated individual harmonic of load voltage (V_{Lh}) (b)Compensated individual harmonic of supply current (I_{Sh})

FIGURE 9. Individual harmonic of compensated system for various cased with series topology.

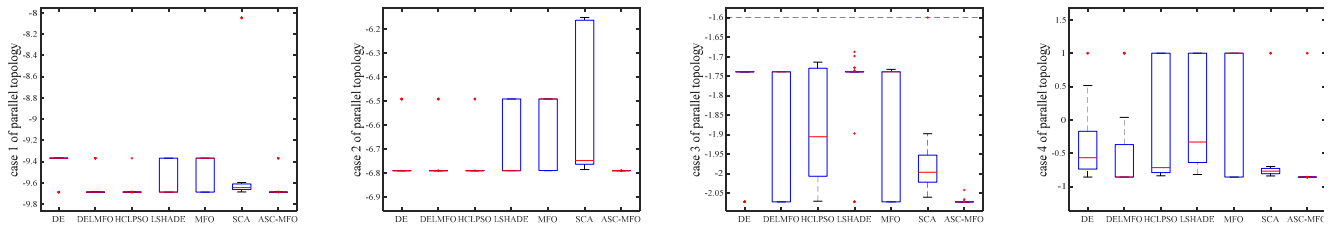

FIGURE 10. Boxplot in 30 runs of different algorithms for four cases of parallel topology.

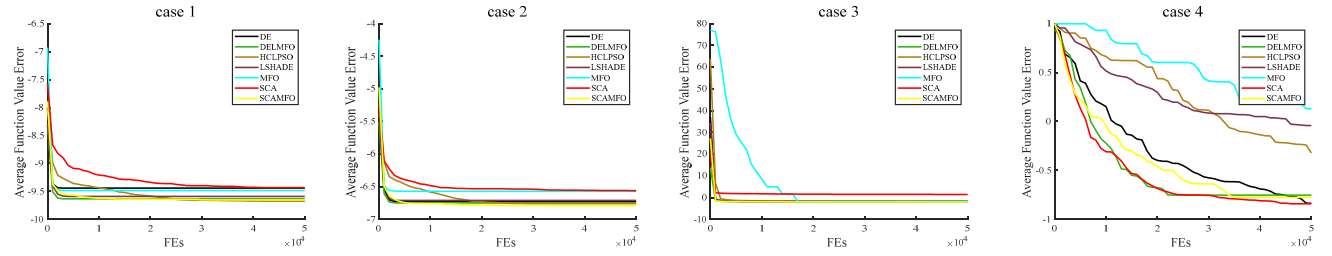

FIGURE 11. Convergence graphs of different algorithms for four cases of parallel topology.

of the proposed ASC-MFO algorithm features unstable; maybe it caused by the proposed subswarm size adaptive mechanism.

Fig.10 and Fig.11 give the boxplot and convergence graphs of different algorithms for four cases of parallel topology, respectively. The same to the results of series topology,

TABLE 5. Comparisons on the statistical results of different algorithms in four cases of parallel topology.

Case number	Algorithm	Objective function value				Total time(s)
		min	mean	max	SD	
case 1	ASC-MFO	-9.6867	-9.6548	-9.3680	9.1E-03	80.2
	SCA	-9.6848	-9.4339	-8.0458	3.0E-01	80.2
	MFO	-9.6867	-9.4848	-9.3680	2.4E-02	69.8
	L-SHADE	-9.6867	-9.5911	-9.3680	2.1E-02	54.8
	HCLPSO	-9.6867	-9.6761	-9.3680	3.3E-03	82.9
	DELMFO	-9.6867	-9.6336	-9.3680	1.4E-02	92.2
	DE	-9.6867	-9.4424	-9.3680	1.8E-02	82.8
case 2	ASC-MFO	-6.7913	-6.7913	-6.7901	5.2E-08	79.6
	SCA	-6.7867	-6.5602	-6.1520	8.0E-02	80.7
	MFO	-6.7913	-6.5719	-6.4921	1.7E-02	70.9
	L-SHADE	-6.7913	-6.7116	-6.4922	1.7E-02	54.5
	HCLPSO	-6.7913	-6.7613	-6.4922	8.0E-03	82.2
	DELMFO	-6.7913	-6.7514	-6.4922	1.0E-02	91.3
	DE	-6.7913	-6.7315	-6.4922	1.4E-02	85.0
case 3	ASC-MFO	-2.0726	-2.0713	-2.0424	3.0E-05	94.4
	SCA	-2.0607	1.4085	100.0000	3.4E+02	81.9
	MFO	-2.0726	-1.8387	-1.7327	2.3E-02	69.6
	L-SHADE	-2.0726	-1.7848	-1.6880	1.4E-02	54.1
	HCLPSO	-2.0711	-1.8759	-1.7145	2.0E-02	82.8
	DELMFO	-2.0726	-1.8724	-1.7389	2.7E-02	90.4
	DE	-2.0726	-1.8168	-1.7389	2.0E-02	84.7
case 4	ASC-MFO	-1.0537	-0.7768	1.0000	4.9E-01	76.14
	SCA	-1.0286	-0.8423	1.0000	2.4E-01	76.66
	MFO	-1.0537	0.1310	1.0000	9.9E-01	68.53
	L-SHADE	-1.0537	-0.0416	1.0000	9.4E-01	48.45
	HCLPSO	-1.0537	-0.7534	1.0000	4.1E-01	80.85
	DELMFO	-1.0537	-0.8363	1.0000	1.9E-01	87.63
	DE	-1.0537	-0.7768	1.0000	4.9E-01	76.14

TABLE 6. Results for case studies with parallel topology.

Parameters	Optimization results using ASC-MFO algorithm			
	case 1	case 2	case 3	case 4
$X_C(\Omega)$	2.7099	2.7013	2.6160	2.6188
$X_L(\Omega)$	104.16	93.31	2.22E-16	0
$K(\Omega)$	20.00	20.00	10.31	8.84
$PF(\%)$	95.00	95.00	95.00	95.00
$DPF(\%)$	95.00	95.03	95.14	95.18
I_S(A)	753.85	753.55	752.89	752.68
V_L(V)	2430.09	2430.80	2431.88	2432.11
$\eta(\%)$	99.30	99.30	99.30	99.30
P_{LOSS}(kW)	12.29	12.28	12.26	12.25
$ITHD(\%)$	0.193	0.500	3.312	3.946
$VTHD(\%)$	0.120	2.708	4.615	5.000
HP (%)	0.227	2.754	5.681	6.370

the lower limit number, upper limit number, lower quartile number, upper quartile number, and the median number of the proposed ASC-MFO algorithm are overlapped in the lowest position, which demonstrates the accuracy and average accuracy of ASC-MFO algorithm. In Fig.11, we can see the proposed ASC-MFO achieves a fast convergence speed and the best convergency value compared to its competitors.

Table 6 gives the optimized results and the calculated value of the series topology by using the proposed ASC-MFO algorithm, and the bar chart of I_{Sh} and V_{Lh} are shown in Fig.12. Compared with the optimization results of the series topology, the results are nearly the same. This is attributed to such the fact that the supply current I_{Sh} in eq (6) and eq (8) and the compensation voltage V_{Lh} in eq (7) and eq (9) are dominant parameters in both two topologies, and other parameters have little effect on them. However, this conclusion is only derived from the medium system and not suitable for all systems. Thus, a specific case study is necessary to determine the parameters character in other systems.

C. EFFECTIVENESS OF INTRODUCED MECHANISMS

In this subsection, some experiments are conducted to verify the effectiveness of our proposed mechanism. *N1* and *N2* represent the exploration group and exploitation

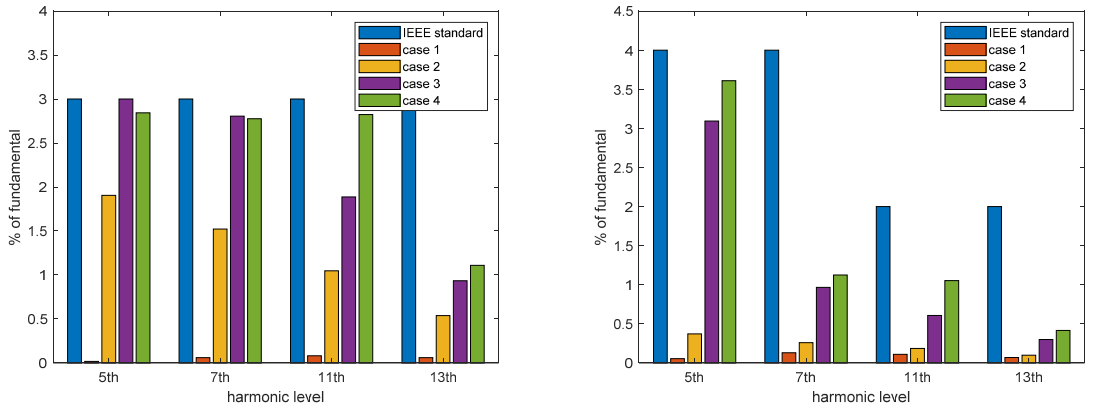

(a) Compensated individual harmonic of load voltage (V_{Lh}) (b) Compensated individual harmonic of supply current (I_{Sh})

FIGURE 12. Individual harmonic of the compensated system for various cased with parral topology.

TABLE 7. Effectiveness test of variable static subswarm size and the proposed adaptive mechanism.

Topology	Case number	Criteria	*N1=0, N2 =50*	*N1=5, N2=45*	*N1=10, N2 =40*	*N1=15, N2=25*	*N1=20, N2 =30*	*N1=25, N2=25*
Series topology	Case 1	Mean	-9.4270	-9.6492	-9.6648	-9.6749	-9.6748	-9.6748
		Std	2.63E-02	7.76E-03	2.91E-03	2.38E-07	2.37E-07	1.43E-06
		Rank	11	9	8	3	4	5
	Case 2	Mean	-6.6023	-6.7793	-6.7842	-6.7847	-6.7848	-6.7847
		Std	2.54E-02	7.23E-04	7.11E-06	4.76E-07	1.60E-07	7.74E-07
		Rank	11	8	5	4	2	3
	Case 3	Mean	-1.8061	-2.0830	-2.0749	-2.0835	-2.0816	1.3193
		Std	1.20E-02	1.22E-04	2.48E-03	4.72E-05	6.79E-05	3.36E+02
		Rank	11	2	6	1	4	12
	Case 4	Mean	-0.3031	-0.1762	-0.5224	-0.5414	-0.8213	-0.6090
		Std	7.61E-01	1.06E+00	8.53E-01	8.64E-01	5.10E-01	7.88E-01
		Rank	11	12	10	9	6	8
Parallel topology	Case 1	Mean	-9.4848	-9.6620	-9.6860	-9.6866	-9.6866	-9.6856
		Std	2.36E-02	5.99E-03	4.93E-06	2.43E-07	5.36E-08	2.18E-05
		Rank	11	9	3	2	1	4
	Case 2	Mean	-6.5719	-6.7702	-6.7911	-6.7912	-6.7911	-6.7905
		Std	1.75E-02	5.55E-03	1.95E-07	7.60E-08	4.34E-07	3.40E-06
		Rank	11	9	3	2	4	5
	Case 3	Mean	-1.8387	-2.0700	1.3329	-2.0717	-2.0723	1.3312
		Std	2.35E-02	5.59E-05	3.36E+02	2.36E-05	5.09E-07	3.36E+02
		Rank	8	5	10	2	1	9
	Case 4	Mean	0.1458	-0.1120	-0.2976	-0.3636	-0.5496	-0.3632
		Std	8.36E-01	8.25E-01	7.22E-01	6.76E-01	4.80E-01	6.76E-01
		Rank	12	11	10	8	7	9
	Average rank		10.75	8.13	6.88	3.88	3.63	6.88
	Final rank		12	10	7	3	2	8
	Best/2nd best/worst		0/0/1	0/1/1	0/0/0	1/3/0	2/1/0	0/0/1

Topology	Case number	Criteria	*N1=30, N2 =20*	*N1=35, N2=15*	*N1=40, N2 =10*	*N1=45, N2=5*	*N1=50, N2 =0*	**ASC-MFO with SAM**
Series topology	Case 1	Mean	-9.6750	-9.6731	-9.6715	-9.6483	-9.3744	-9.6750
		Std	9.15E-09	4.01E-05	4.39E-05	1.34E-03	2.95E-01	5.17E-08
		Rank	2	6	7	10	12	1
	Case 2	Mean	-6.7831	-6.7818	-6.7629	-6.7187	-6.4772	-6.7849
		Std	3.74E-05	3.87E-05	9.81E-03	1.54E-02	7.04E-02	3.68E-07
		Rank	6	7	9	10	12	1
	Case 3	Mean	-2.0827	-2.0785	-2.0628	-2.0463	-1.9845	-2.0408
		Std	3.90E-05	7.58E-04	1.66E-03	2.26E-03	6.77E-03	1.17E-02
		Rank	3	5	7	8	10	9
	Case 4	Mean	-0.8915	-0.8820	-0.9399	-0.7810	-0.9424	-1.0319
		Std	3.98E-01	3.94E-01	2.75E-01	4.90E-01	1.31E-01	1.42E-01
		Rank	4	5	3	7	2	1
Parallel topology	Case 1	Mean	-9.6847	-9.6837	-9.6817	-9.6733	-9.4339	-9.6548
		Std	7.85E-05	9.27E-05	1.26E-04	2.07E-04	2.96E-01	9.14E-03
		Rank	5	6	7	8	12	10
	Case 2	Mean	-6.7904	-6.7895	-6.7886	-6.7630	-6.5602	-6.7913
		Std	1.43E-05	3.87E-05	1.95E-05	1.30E-03	8.04E-02	5.19E-08
		Rank	6	7	8	10	12	1
	Case 3	Mean	-2.0706	1.3370	-2.0606	-2.0257	1.4085	-2.0713
		Std	6.47E-05	3.36E+02	2.82E-04	2.35E-03	3.35E+02	3.02E-05
		Rank	4	11	6	7	12	3
	Case 4	Mean	-0.7354	-0.5861	-0.6016	-0.7424	-0.6001	-0.7356
		Std	2.15E-01	3.92E-01	3.95E-01	1.13E-01	2.86E-01	2.15E-01
		Rank	3	6	4	1	5	2
	Average rank		4.13	6.63	6.38	7.63	9.63	3.5
	Final rank		4	6	5	9	11	1
	Best/2nd best/worst		0/1/0	0/0/0	0/0/0	1/0/0	0/1/5	4/1/0

group size, respectively. The number of subpopulations is 5 in step, changing from 0 to 50. Note the condition $N1 = 0$, $N2 = 50$, and $N1 = 50$, $N2 = 0$ represents the SCA algorithm and MFO algorithm, respectively. Hybrid conditions

only change the subswarm size without using our proposed adaptive mechanism. Condition ASC-MFO is our complete proposed algorithm. It can be derived from Table 7 that all hybrid conditions with static swarm size ranked better than both the SCA algorithm (ranked 12) and the MFO algorithm (ranked 11), which demonstrates that the SCA algorithm introduced into MFO algorithm improves the performance in this optimization task. Besides, subswarm size $N1 = 20$, $N2 = 30$ (ranked 2) ranked first among the hybrid conditions. Moreover, the proposed ASC-MFO algorithm with SAM ranked first in this test and obtained four first rank and a second-first rank in 8 specific case studies, which proves proposed SAM can significantly improve the performance of ASC-MFO without SAM strategy, and the SAM strategy is an irreplaceable strategy in the proposed ASC-MFO algorithm.

VI. CONCLUSION AND FUTURE WORK

The objective function of HAPF is considered multimodal with local optima. Thus, it is tricky for a large number of state-of-art algorithms to obtain accurate parameters of the HAPF. This paper proposed a new MFO variant named adaptive sine-cosine moth-flame algorithm (ASC-MFO) to design the two topologies of HAPF, i.e., series topology and parallel topology. Experimental results indicate that when compared with other state-of-art meta-heuristic algorithms, the proposed ASC-MFO algorithm can obtain better performance in the problem of designing HAPF, especially in terms of accuracy, average accuracy, and reliability. This can be attributed to the following facts: the swarm division into two subswarms i.e., exploitation group and the exploration group successfully preserve the diversity of the population, which balance the exploitation ability and the exploration ability of the ASC-MFO algorithm; the PFG strategy and The HEG strategy successfully enhance the exploitation and the exploration ability of the exploitation group and exploration group, respectively. The implement of these two strategies can further balance the exploitation ability and the exploration ability of the proposed ASC-MFO algorithm; our proposed SAM can precisely adjust the swarm size in every single generation, which ensures that the exploitation ability and the exploration ability of the ASC-MFO in each generation are well balanced.

However, since the parameters of the ASC-MFO algorithm are set according to experience, the ASC-MFO algorithm proposed is still worthy of further improvement in terms of parameter adjustment. In the future, some adaptive parameter mechanisms will be developed to address this problem. Moreover, the proposed ASC-MFO will be used to analyze other cases of HAPF in the power system or settle some other multi-objective and constrained problems. Furthermore, some other meta-heuristic algorithms will be proposed to solve optimization problems in the power system.

ACKNOWLEDGMENT

(Yufan Wu and Chunquan Li contributed equally to this work.)

REFERENCES

[1] R. L. de Araujo Ribeiro, C. C. de Azevedo, and R. M. de Sousa, "A robust adaptive control strategy of active power filters for power-factor correction, harmonic compensation, and balancing of nonlinear loads," *IEEE Trans. Power Electron.*, vol. 27, no. 2, pp. 718–730, Feb. 2012.

[2] H. Wen, Z. Teng, Y. Wang, and X. Hu, "Spectral correction approach based on desirable sidelobe window for harmonic analysis of industrial power system," *IEEE Trans. Ind. Electron.*, vol. 60, no. 3, pp. 1001–1010, Mar. 2013.

[3] M. T. Elmathana, A. F. Zobaa, and S. H. E. Abdel Aleem, "Economical design of multiple-arm passive harmonic filters for an industrial firm–Case study," in *Proc. IEEE 15th Int. Conf. Harmon. Qual. Power*, Jun. 2012, pp. 438–444.

[4] K. Nikum, A. Wagh, R. Saxena, and B. Mishra, "New economical design of SVC and passive filters to improve power quality at railway substation: A case study," *J. Inst. Eng. (India): B*, vol. 100, no. 5, pp. 529–540, Oct. 2019.

[5] D. Zhao, W. Liu, K. Shen, G. Zhao, and X. Wang, "Multi-objective optimal design of passive power filter for aircraft starter/generator system application," *J. Eng.*, vol. 2018, no. 13, pp. 636–641, Jan. 2018.

[6] A. Karadeniz and M. E. Balci, "Comparative evaluation of common passive filter types regarding maximization of transformer's loading capability under non-sinusoidal conditions," *Electr. Power Syst. Res.*, vol. 158, pp. 324–334, May 2018.

[7] H. Akagi, "New trends in active filters for power conditioning," *IEEE Trans. Ind. Appl.*, vol. 32, no. 6, pp. 1312–1322, Nov./Dec. 1996.

[8] A. K. Jindal, A. Ghosh, and A. Joshi, "The protection of sensitive loads from interharmonic currents using shunt/series active filters," *Electric Power Syst. Res.*, vol. 73, no. 2, pp. 187–196, Feb. 2005.

[9] S. H. E. A. Aleem, A. F. Zobaa, and M. M. A. Aziz, "Optimal *C*-type passive filter based on minimization of the voltage harmonic distortion for nonlinear loads," *IEEE Trans. Ind. Electron.*, vol. 59, no. 1, pp. 281–289, Jan. 2012.

[10] K. Yu, J. J. Liang, B. Y. Qu, Z. Cheng, and H. Wang, "Multiple learning backtracking search algorithm for estimating parameters of photovoltaic models," *Appl. Energy*, vol. 226, pp. 408–422, Sep. 2018.

[11] H. Duan, P. Li, Y. Shi, X. Zhang, and C. Sun, "Interactive learning environment for bio-inspired optimization algorithms for UAV path planning," *IEEE Trans. Educ.*, vol. 58, no. 4, pp. 276–281, Nov. 2015.

[12] Y.-J. Gong, J.-J. Li, Y. Zhou, Y. Li, H. S.-H. Chung, Y.-H. Shi, and J. Zhang, "Genetic learning particle swarm optimization," *IEEE Trans. Cybern.*, vol. 46, no. 10, pp. 2277–2290, Oct. 2016.

[13] L. Gong, W. Cao, and J. Zhao, "An improved PSO algorithm for high accurate parameter identification of PV model," in *Proc. IEEE Int. Conf. Environ. Electr. Eng. IEEE Ind. Commercial Power Syst. Eur. (EEEIC/I&CPS Europe)*, Jun. 2017, pp. 1–5.

[14] C. Li, Z. Niu, Z. Song, B. Li, J. Fan, and P. X. Liu, "A double evolutionary learning moth-flame optimization for real-parameter global optimization problems," *IEEE Access*, vol. 6, pp. 76700–76727, 2018.

[15] S. Mahaboob, S. K. Ajithan, and S. Jayaraman, "Optimal design of shunt active power filter for power quality enhancement using predator-prey based firefly optimization," *Swarm Evol. Comput.*, vol. 44, pp. 522–533, Feb. 2019.

[16] A. K. Tiwari and S. P. Dubey, "Ant colony optimization based hybrid active power filter for harmonic compensation," in *Proc. Int. Conf. Electr., Electron., Optim. Techn. (ICEEOT)*, Mar. 2016, pp. 777–782.

[17] Y.-P. Chang and C.-N. Ko, "A PSO method with nonlinear time-varying evolution based on neural network for design of optimal harmonic filters," *Expert Syst. Appl.*, vol. 36, no. 3, pp. 6809–6816, Apr. 2009.

[18] Y.-P. Chang and C. Low, "An ant direction hybrid differential evolution heuristic for the large-scale passive harmonic filters planning problem," *Expert Syst. Appl.*, vol. 35, no. 3, pp. 894–904, Oct. 2008.

[19] Y.-P. Chang, C. Low, and S.-Y. Hung, "Integrated feasible direction method and genetic algorithm for optimal planning of harmonic filters with uncertainty conditions," *Expert Syst. Appl.*, vol. 36, no. 2, pp. 3946–3955, Mar. 2009.

[20] M. Mohammadi, "Bacterial foraging optimization and adaptive version for economically optimum sitting, sizing and harmonic tuning orders setting of LC harmonic passive power filters in radial distribution systems with linear and nonlinear loads," *Appl. Soft Comput.*, vol. 29, pp. 345–356, Apr. 2015.

[21] N. He, L. Huang, J. Wu, and D. Xu, "Multi-objective optimal design for passive part of hybrid active power filter based on particle swarm optimization," *Proc. CSEE*, vol. 27, no. 0258-8013, p. TN713.8, Sep. 2008.

[22] P. P. Biswas, P. N. Suganthan, and G. A. J. Amaratunga, "Minimizing harmonic distortion in power system with optimal design of hybrid active power filter using differential evolution," *Appl. Soft Comput.*, vol. 61, pp. 486–496, Dec. 2017.
[23] S. Mirjalili, "Moth-flame optimization algorithm: A novel nature-inspired heuristic paradigm," *Knowl.-Based Syst.*, vol. 89, pp. 228–249, Nov. 2015.
[24] M. A. E. Aziz, A. A. Ewees, and A. E. Hassanien, "Whale optimization algorithm and moth-flame optimization for multilevel thresholding image segmentation," *Expert Syst. Appl.*, vol. 83, pp. 242–256, Oct. 2017.
[25] M. Talaat, A. S. Alsayyari, M. A. Farahat, and T. Said, "Moth-flame algorithm for accurate simulation of a non-uniform electric field in the presence of dielectric barrier," *IEEE Access*, vol. 7, pp. 3836–3847, 2019.
[26] G. M. Soliman, M. Khorshid, and T. H. Abou-El-Enien, "Modified moth-flame optimization algorithms for terrorism prediction," *Int. J. Appl. Innov. Eng. Manage.*, vol. 5, no. 7, pp. 47–58, 2016.
[27] Z. Li, Y. Zhou, S. Zhang, and J. Song, "Lévy-flight moth-flame algorithm for function optimization and engineering design problems," *Math. Problems Eng.*, vol. 2016, Aug. 2016, Art. no. 1423930.
[28] D. H. Wolpert and W. G. Macready, "No free lunch theorems for optimization," *IEEE Trans. Evol. Comput.*, vol. 1, no. 1, pp. 67–82, Apr. 1997.
[29] S. Mirjalili, "SCA: A sine cosine algorithm for solving optimization problems," *Knowl.-Based Syst.*, vol. 96, pp. 120–133, Mar. 2016.
[30] *IEEE Recommended Practices and Requirements for Harmonic Control in Electrical Power Systems*, IEEE Ind. Appl. Soc./Power Eng. Soc., Inst. Elect. Electron. Eng., Inc., New York, NY, USA, 1993.
[31] F. Z. Peng, H. Akagi, and A. Nabae, "A new approach to harmonic compensation in power systems–A combined system of shunt passive and series active filters," *IEEE Trans. Ind. Appl.*, vol. 26, no. 6, pp. 983–990, Nov./Dec. 1990.
[32] A. F. Zobaa, "Optimal multiobjective design of hybrid active power filters considering a distorted environment," *IEEE Trans. Ind. Electron.*, vol. 61, no. 1, pp. 107–114, Jan. 2014.
[33] R. Tanabe and A. S. Fukunaga, "Improving the search performance of SHADE using linear population size reduction," in *Proc. IEEE Congr. Evol. Comput. (CEC)*, Jul. 2014, pp. 1658–1665.
[34] N. Lynn and P. N. Suganthan, "Heterogeneous comprehensive learning particle swarm optimization with enhanced exploration and exploitation," *Swarm Evol. Comput.*, vol. 24, pp. 11–24, Oct. 2015.
[35] R. Storn and K. Price, "Differential evolution-a simple and efficient heuristic for global optimization over continuous spaces," *J. Global Optim.*, vol. 11, no. 4, pp. 341–359, 1997.

YUFAN WU is currently pursuing the B.Sc. degree with the School of Information Engineering, Nanchang University, Nanchang, China.

His current research interests include optimization problems, swarm optimization algorithms, and other computational intelligence techniques.

RONGLING CHEN received the B.Sc. degree from Nanchang University, Nanchang, China, in 1995, and the M.Sc. degree from the Institute of Modern Physics, Chinese Academy of Sciences, Lanzhou, China, in 1998.

She has been with the School of Information Engineering, Nanchang University, since 1998, where she is currently a Lecturer. She has also interested in computational intelligence.

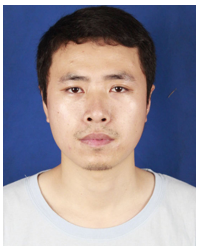

CHUNQUAN LI (Member, IEEE) received the B.Sc. M.Sc., and Ph.D. degrees from Nanchang University, Nanchang, China, in 2002, 2007, and 2015, respectively.

He has been with the School of Information Engineering, Nanchang University, since 2002, where he is currently a Professor and a Young Scholar of Ganjiang River. He is also a Visiting Professor with the Department of Systems and Computer Engineering, Carleton University, Ottawa, ON, Canada. He has published over 30 research articles. His current interests include computing intelligence, haptics, virtual surgery simulation, robotics, and their applications to biomedical engineering.

LEYINGYUE ZHANG is currently pursuing the B.Sc. degree with the School of Information Engineering, Nanchang University, Nanchang, China.

Her current research interests include particle swarm optimization, moth-flame optimization, and other computational intelligence techniques.

WANXUAN DAI is currently pursuing the degree with the School of Information Engineering, Nanchang University, Nanchang, Jiangxi, China.

His current research interests include swarm particle swarm optimization, genetic algorithms, and other computational intelligence techniques.